

Experimental Study on the Aerodynamic Performance of Autonomous Boat with Wind Propulsion and Solar Power

Joga Dharma Setiawan^{1,2}

¹Mechanical Engineering Department
Universitas Diponegoro
Semarang, Indonesia

²National Center for Sustainable
Transportation Technology, Indonesia
joga.setiawan@ft.undip.ac.id

Bentang Arief Budiman^{1,2}

¹Faculty of Mechanical and Aerospace
Engineering

Institut Teknologi Bandung, Indonesia
²National Center for Sustainable
Transportation Technology, Indonesia
bentang@ftmd.itb.ac.id

Mochammad Ariyanto^{1,2}

¹Mechanical Engineering Department
Universitas Diponegoro
Semarang, Indonesia

²National Center for Sustainable
Transportation Technology, Indonesia
mochammad_ariyanto@ft.undip.ac.id

Trias Andromeda^{1,2}

¹Electrical Engineering Department
Universitas Diponegoro
Semarang, Indonesia

²National Center for Sustainable
Transportation Technology, Indonesia
trias1972@yahoo.com

Deddy Chrismianto

Naval Architecture Department
Universitas Diponegoro
Semarang, Indonesia

deddychrismianto@yahoo.co.id

Muhamad Abdul Aziz

Mechanical Engineering Department
Universitas Diponegoro
Semarang, Indonesia
azizaspire@gmail.com

Abstract— The autonomous boat in this research has the capability of using fully renewable energy sources in which its wing sail can provide aerodynamic forces for propulsion while the solar cells provide the power for control and communication systems. Thus, this boat can operate in a long duration, suitable for ocean research and monitoring missions. Similar to an airplane wing, the design of the wing sail is taken from NACA 0018 that can provide good performance in low Reynolds-number. The purpose of this study is to experimentally study the aerodynamic performance of a 1/4th scale wing sail by varying the flap angle in a laboratory set-up. The aerodynamic of wing sail produces lift and drag forces that depend on the wing sail angle of attack. In this study, an encoder is used to measure the angle of attack of wing sail, a potentiometer for measuring the flap angle, and an anemometer for measuring the wind speed. A servo motor is used for controlling the flap angle. The digital data acquisition uses Arduino Uno as the microcontroller which is wired to a PC and coded in MATLAB/Simulink using Arduino package. The experiment results show the wing sail performance, the effect varying flap angles. The total aerodynamic forces were generated in this experiment.

Keywords—Wing sail, wind propulsion, autonomous boat.

I. INTRODUCTION

An autonomous sailboat has the advantage of low energy consumption. Wing sail can provide aerodynamic forces that can be used for sailing as shown in Fig. 1. Similar to an airplane wing, the design of the wing sail is taken from NACA 0018 that can provide good performance in low Reynolds-number. Wing sail work with air that passes through such that the wing has kinetic energy to provide lift and drag forces to propel a sailboat. Thus, the boat needs electrical energy only to control the sail through a servo motor driving the flap. The flap is used to control the angle of attack, α of the wing sail to propel boat correctly. The autonomous sailboat is being developed for future ocean research activities. The sailboat may have the capability for long mission ranges, carrying many sensors, functioning as a low-cost ocean observation platform, and providing real-time

data transmission similar to the previous studies by Alves et.al and Tretow [1, 2].

To propel sailboat precisely, the flap angle must operate quickly and accurately, therefore the lift force, L_w that wing sail generates must be in the right direction. The flap angle, δ_{flap} is actuated by a servo motor that can be commanded by a radio remote control transmitter. An experiment was conducted using an electric fan to produce airflow (V_A) to propel wing sail at various flap angle, δ_{flap} . The wind speed is recorded by an anemometer. The feedback potentiometer system in servomotor was used to determine the flap angle (δ_{flap}). The angle of attack (α) of the wing sail was measured by a 10-bit rotary encoder.

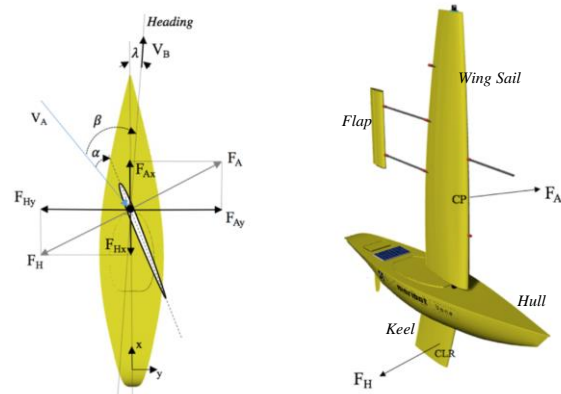


Fig. 1. The forces acting on a sailboat [2]

II. METHODS OF WING SAILING AND DATA ACQUISITION

A. Wing Sailing

Moving air has kinetic energy that can interact with wing sail causing a pressure difference between the opposite side of the wing surface and then creating aerodynamic force, a lift force, L_w [3]. This lift force has a direction perpendicular to the airflow, while the drag force, D_w is in the direction of the airflow. Both of these forces are strongly influenced by

air density, airfoil area and wind speed [4]. On the other hand, hydrodynamic force interaction will occur on the hull. The forces acting on the sailboat can be seen in Fig. 1. The aerodynamic force is used to produce thrust while the hull and keel are used to steer the ship in the desired path when sailing.

The flap angle, δ_{flap} will create a moment on the vertical axis and make the wing sail rotate into the air stream with an angle of attack, α as shown in Fig. 2. The angle of attack is positively defined clockwise from the direction of the incoming wind.

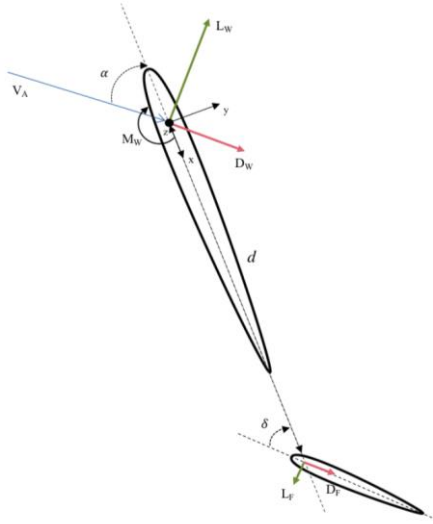


Fig. 2. Forces on the wing sail and flap [3]

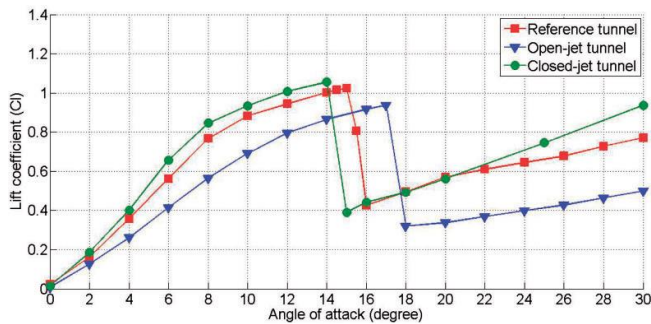


Fig. 3. Lift coefficient for NACA 0018 [5]

The center of pressure is the point where the resultant vector of lift L_W and drag D_W works. Because the wing moves freely, the wing will move until the equilibrium moment occurs at the pivot point. Then this will place the center of pressure (CP) at the same vertical point on rotation on the z -axis where the moment of the wing sail, M_W is zero. The function of the flap is to make the flap moment, M_R which is used to make the wing rotate to a certain angle of attack, α . The attack angle of the wing sail with NACA 0018 has a lift coefficient configuration on the as shown in Fig. 3.

B. Servomotor

This experiment uses the servo motor Tower Pro MG995. Giving PWM (Pulse Width Modulation) to the servo motor will make the flap rotate to a certain position and stop. The

servo motor terminal port consists of 3 parts: V_{cc} , Gnd, and Control. This servomotor was modified to get the angular position of the servo motor using a potentiometer that is already in the servo motor as shown in Fig.4. The signal from the potentiometer is then used to acquire the flap angle.

C. Rotary Encoder

In this experiment, an absolute encoder shown in Fig. 5 is chosen. The number of bits in the binary number will correspond to the number of lines. In an encoder that has 10 lines, there will be 10 bits and there are 2^{10} positions that can be detected, namely 1024 with a resolution of $360/1024 = 0.35^\circ$. The encoder is used to measure the angle of the wing sail.

D. Time response

The output of a dynamical system is the sum of two responses the forced response and the natural response [6]. In time-domain, the rise time, T_R is defined as the time for the response to go from 0.1 to 0.9 of its final value [7]. The rise time of the wing sail will be used as the parameter in determining the performance of the wing sail at various flap lever arm distance, d and the amplitude of the actuated flap angle, δ_{flap} .

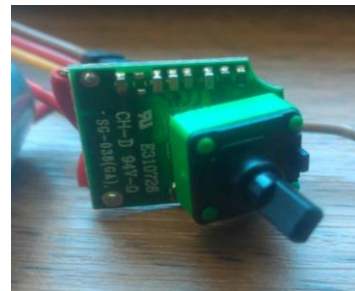


Fig. 4. Potentiometer in servomotor TowerPro MG995



Fig. 5. Rotary Encoder HAN18U5VA1

E. Scaled-Model Parameter

The scaled-model shown in Fig. 6 is the finished product of the wing sail and flap with considerations that have been made in the previous research study [3]. The wing has the solar cells on both sides to capture the sun energy needed for communication and control systems. The aspect ratio (AR) can be calculated using Equation 1 while then taper ratio, t_{ratio} is determined using Equation 2, and flap size ratio (% flap size) is found using Equation 3. The parameter values of the wing sail are shown in Table 1.

$$AR = \frac{2b}{c_r + c_t} \quad (1)$$

$$t_{ratio} = \frac{c_t}{c_r} \quad (2)$$

$$\% \text{ flap size} = \frac{A_{flap}}{A_{wing}} \quad (3)$$

Using the parameters in Table 1 and the results of comparison testing with the vortex lattice method (VLM), the values of the lift and drag coefficients can be found [3]. For $AR = 5.31$, C_L is 0.934 and C_D is 0.029. At $t_{ratio} = 0.48$ then $C_L = 0.903$. For $\% \text{ flap size} = 11.2\%$ then $C_L = 0.928$. Afterward $\% \text{ rotational axis position} = 26.6\%$ then $C_L = 0.904$ and the normalized stability derivative = 2.02. These values are taken to show that the wing sail values are in good range.

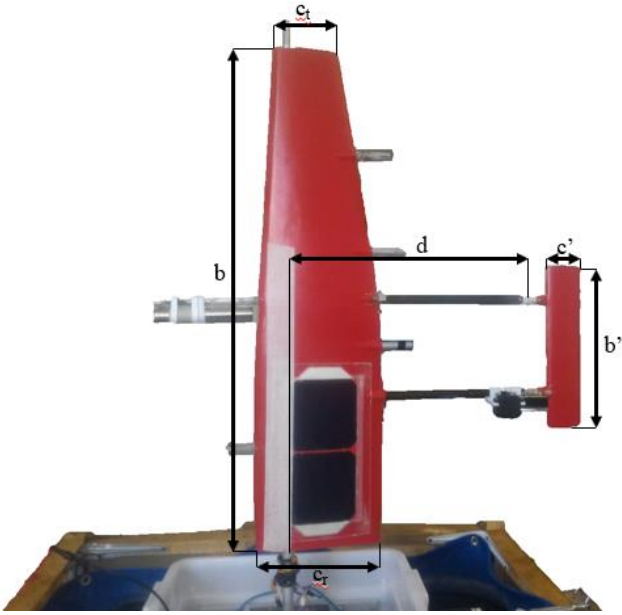


Fig. 6. Scaled-model wing sail and flap for autonomous sailboat

TABLE I. WING SAIL SPECIFICATION

Parameter	Value
Wing span, b	89 cm
Flap lever arm, d	44.5 cm
Tip chord, c_t	11 cm
Root chord, c_r	22.5 cm
Flap span, b'	30.7 cm
Flap chord, c'	6.6 cm
Aspect ratio (AR)	5.31
Taper ratio, t_{ratio}	0.48
The ratio between wing and flap (% flap size)	11.2 %
Distance between wing sail shaft and the tip of wing chord (% rotational axis position)	26.6 %

F. Experimental Setup

As shown in Fig. 7, four portable load cells, labeled as “L”, are mounted on each side of the square shape of the hull of the scaled-model to measure the resulting aerodynamic forces. In general, there are nine main components needed to conduct the experiment as shown in Fig. 8. A power supply is needed to power all sensors and actuators. The sensors are a rotary encoder to measure the wing sail angle of attack, α , a potentiometer to measure the flap angle, δ_{flap} , and an anemometer to measure the wind speed, V_A coming from the electric fan. The signal available at the potentiometer was found to be quite noisy such that a lowpass filter was needed. Furthermore, the actuator to move the flap is the servomotor, to move it requires a PWM (Pulse width modulation) signal which is generated by the Radiolink AT9S remote control to be received by the Radiolink R9DS receiver connected to the servomotor. All of these sensors are connected to Arduino Uno which is then connected to a PC. The data acquisition and command were done in Matlab/Simulink with Arduino library.

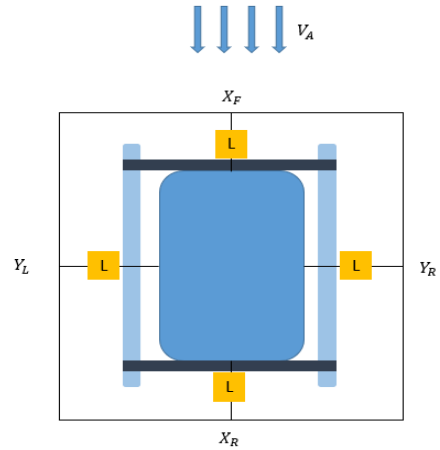


Fig. 7. Top view sketch from experiment model

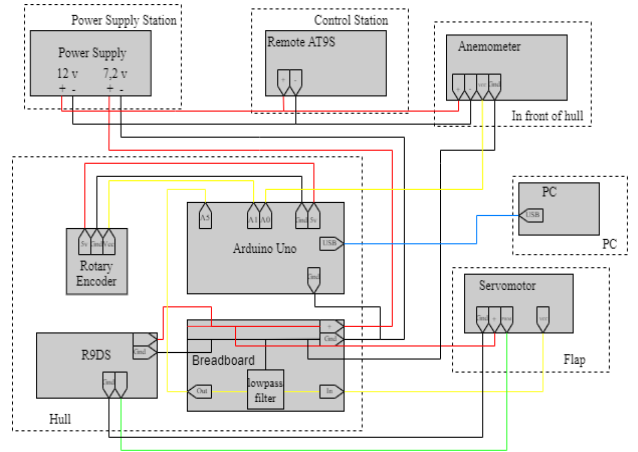


Fig. 8. Schematic diagram of the experiment setup

In the experiment, Matlab/Simulink with Arduino Library is used for data acquisition as shown in Fig. 9 with a sampling rate of 0.01 s. The wing sail must be able to freely rotate at 360° . The wing sail angle of attack, α is measured using a 10-bit rotary encoder. Equations 4 and 5 are used to convert them to 360° scale. The potentiometer is used for the flap angle, δ_{flap} measurement. During calibration, Equation 6 is used for converting the voltage from the potentiometer into the unit in degree. The anemometer is calibrated with a

portable anemometer to find the wind speed, V_A using Equation 7 to. S in equations 5 to 7 means the signal output. This experiment can be categorized to hardware-in-the-loop simulation (HILS) [8].

The zero value for the wing sail angle of attack is inline with the longitudinal axis of the sailboat model while the zero value for the flap angle, δ_{flap} is in line with the flap lever arm, d . The wing sail angle of attack, α and the flap angle, δ_{flap} are positive directions when they rotate clockwise as shown in Fig. 10.

III. EXPERIMENT RESULT AND ANALYSIS

A. Effects of Flap angle

The first experiment was conducted to obtain the relation between the flap angle, δ_{flap} , and the wing sail angle of attack, α . This experiment requires at least 15 s duration in order to reach a settling time in each test. During the test, the wing sail is given airflow, V_A from the fan. The results are averaged and shown in Fig. 11. It can be seen in Fig. 11 that the data generated is not linear. The wing sail tends to an angle of attack, α negative at the flap angle, $\delta_{flap} = 0^\circ$. This may happen that actual shape of the wing sail is not symmetrical during fabrication. The maximum angle of attack, α is 20.64° at the flap angle $\delta_{flap} = -12^\circ$ while the maximum angle of attack, α is -20.40° at the flap angle, $\delta_{flap} = 12^\circ$.

$$360 \text{ deg} = \frac{360^\circ}{1023} \quad (4)$$

$$\alpha = S_{encoder} - 172.8 \quad (5)$$

$$\delta = -0.3083 S_{potentiometer} + 108.5 \quad (6)$$

$$V_A = 0.0219 S_{Anemometer} - 0.0631 \quad (7)$$

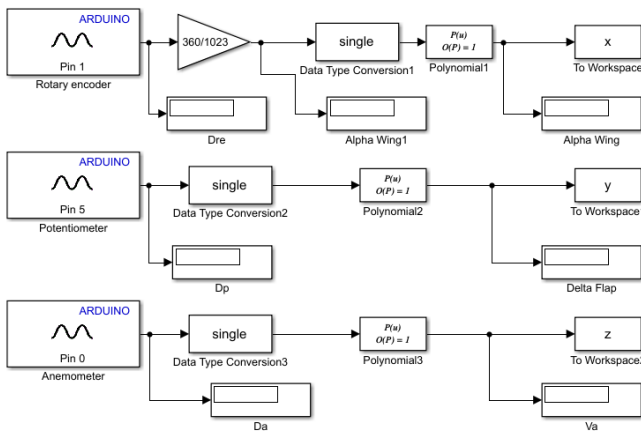


Fig. 9. Simulink experimental diagram

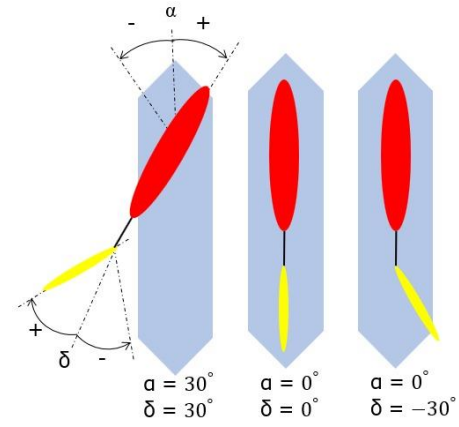


Fig. 10. Example an angle of attack of wing sail and flap angle

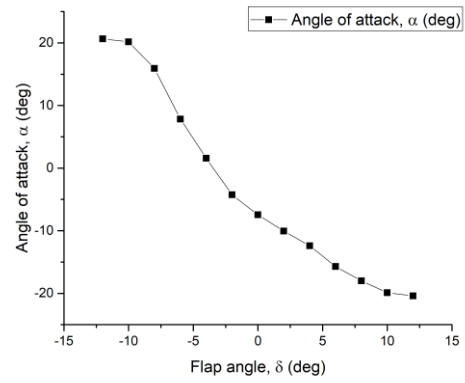


Fig. 11. The relation between the flap angle, δ_{flap} , and the wing sail angle of attack, α

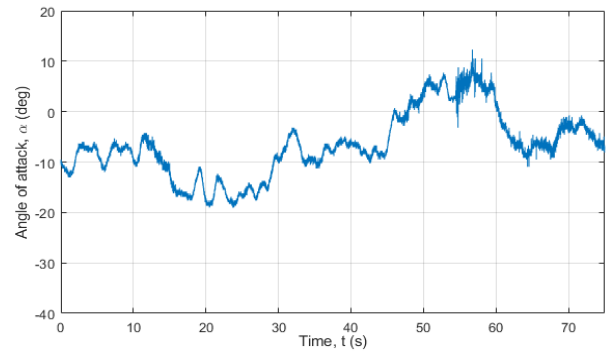


Fig. 12. Wing angle of attack at $\delta_{flap} = \pm 5^\circ$ and $d = 44.5$ cm

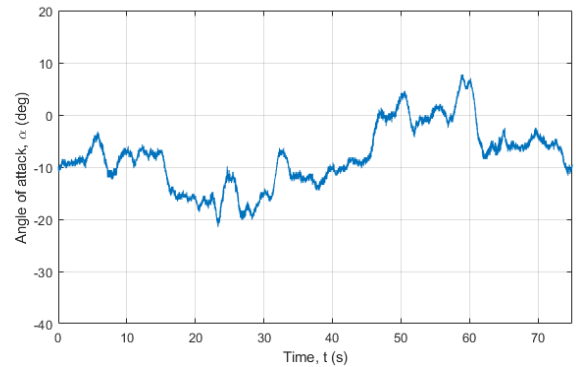


Fig. 13. Wing angle of attack at $\delta_{flap} = \pm 5^\circ$ and $d = 50$ cm

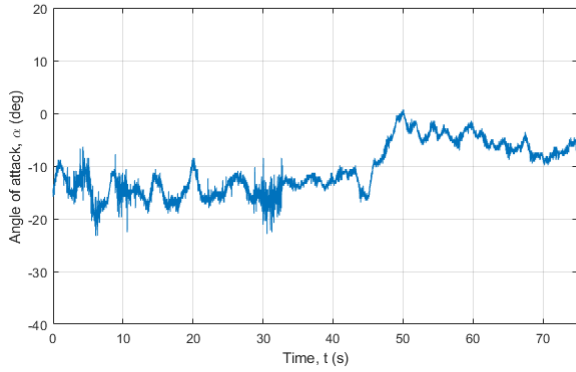


Fig. 14. Wing angle of attack at $\delta_{\text{flap}} = \pm 5^\circ$ and $d = 55$ cm

B. Effects of Time Response

This simulation process is carried out dynamically by moving the flap from the flap angle, $\delta_{\text{flap}} 0^\circ \rightarrow \delta_{\text{flap}}$ positive, δ_{flap} positive $\rightarrow \delta_{\text{flap}} 0^\circ$, $0^\circ \rightarrow \delta_{\text{flap}}$ negative, and the flap angle from δ_{flap} negative $\rightarrow 0^\circ$, for δ_{flap} positive $\rightarrow \delta_{\text{flap}} 0^\circ$ will not be analyzed. The commanded flap angle, δ_{flap} configuration used in testing is in the form of a square signal with the amplitude of $\pm 5^\circ$, $\pm 10^\circ$, and $\pm 15^\circ$. During testing the responses of the wing sail angle of attack are evaluated at various lengths of the flap lever arm, $d = 44.5$ cm, 50 cm, and 55 cm. The test was carried out with a duration of 75 s where the change of δ_{flap} is at every 15 s. Figs. 12-14 show the result of the experiment with the amplitude of the flap angle, $\delta_{\text{flap}} = \pm 5^\circ$. Figs. 15-17 show the result of the experiment with $\delta_{\text{flap}} = \pm 10^\circ$ while Figs. 20-22 show the result of the experiment with $\delta_{\text{flap}} = \pm 15^\circ$.

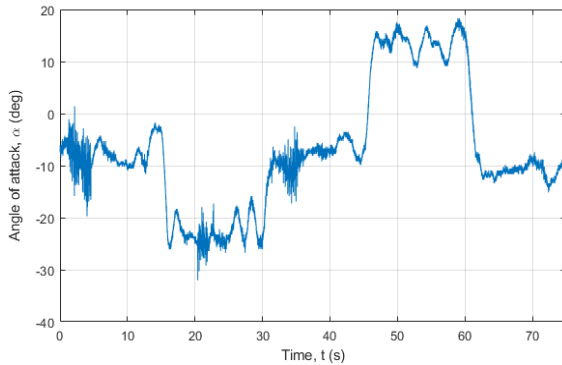


Fig. 15. Wing angle of attack at $\delta_{\text{flap}} = \pm 10^\circ$ and $d = 44.5$ cm

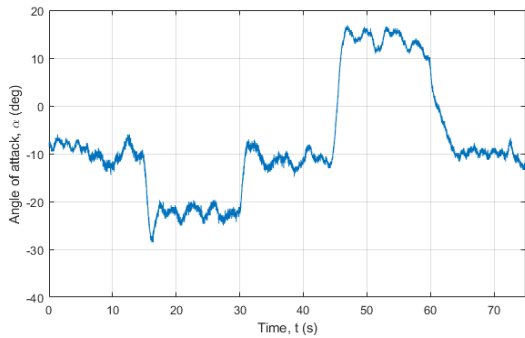


Fig. 16. Wing angle of attack at $\delta_{\text{flap}} = \pm 10^\circ$ and $d = 50$ cm

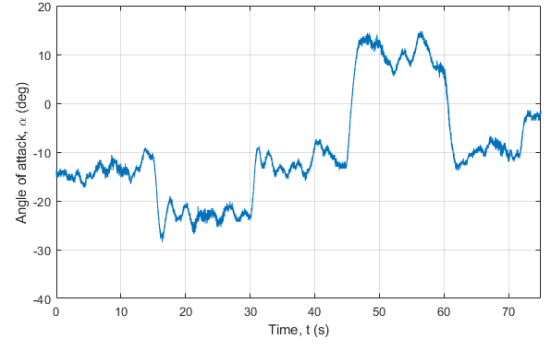


Fig. 17. Wing angle of attack at $\delta_{\text{flap}} = \pm 10^\circ$ and $d = 55$ cm

Fig. 21 recaps the results of the rise time, T_R from the results in Figs. 12-14 for $\delta_{\text{flap}} = \pm 5^\circ$. It can be seen there is a conflicting performance of the responses. At $\delta_{\text{flap}} = 5^\circ$, the longer the flap lever arm, d , the lower is T_R in which the lowest value is at $d = 55$ cm with $T_R = 0.76$ s. While at $\delta_{\text{flap}} = -5^\circ$ the longer the flap lever arm, d , the higher is T_R in which the lowest value is at $d = 44.5$ cm with $T_R = 0.87$ s. Then $\delta_{\text{flap}} = 0^\circ$ the lowest value is at $d = 55$ cm with $T_R = 1.58$ s. Fig. 22 recaps the results of the rise time, T_R from the results in Figs. 15-17 for $\delta_{\text{flap}} = \pm 10^\circ$. It can be seen there is a conflicting performance of the responses. At $\delta_{\text{flap}} = 10^\circ$, lowest value is at $d = 50$ cm with $T_R = 0.42$ s. While at $\delta_{\text{flap}} = -10^\circ$ the longer the flap lever arm, $d = 44.5$ cm with $T_R = 1.02$ s. Then $\delta_{\text{flap}} = 0^\circ$ the lowest value is at $d = 55$ cm with $T_R = 1.21$ s. Fig. 23 recaps the results of the rise time, T_R from the results in Figs. 18-20 for $\delta_{\text{flap}} = \pm 15^\circ$. It can be seen there is a conflicting performance of the responses. At $\delta_{\text{flap}} = 15^\circ$, lowest value is at $d = 44.5$ cm with $T_R = 0.54$ s. While at $\delta_{\text{flap}} = -15^\circ$ the longer the flap lever arm, $d = 55$ cm with $T_R = 0.5$ s. Then $\delta_{\text{flap}} = 0^\circ$ the lowest value is at $d = 50$ cm with $T_R = 0.92$ s. Based on theoretical the longer the flap lever arm, d , the higher is T_R . Inconsistencies in the time response may be caused by the unsteadiness of the wind produced by the electric fan and inaccuracies in fabrication of the wing sail and the construction of the test bench.

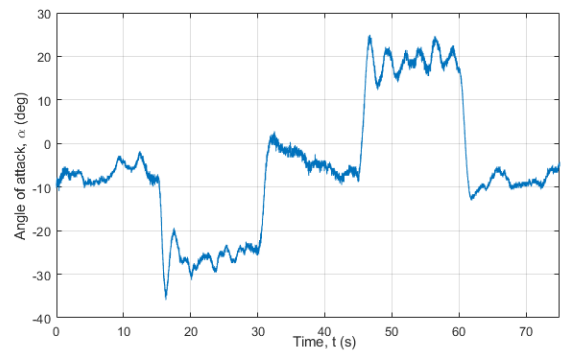


Fig. 18. Wing angle of attack at $\delta_{\text{flap}} = \pm 15^\circ$ and $d = 44.5$ cm

C. Effects of Lift and Drag Force

Fig. 24 shows the results of measurement using four portable load cells. By varying the angle of attack, α to -20° , -15° , -10° , -5° , 5° , 10° , 15° , dan 20° . This experiment result shows an almost symmetrical curve of the resultant values namely F_R obtained from the lift force, L_W and the drag force, D_W .

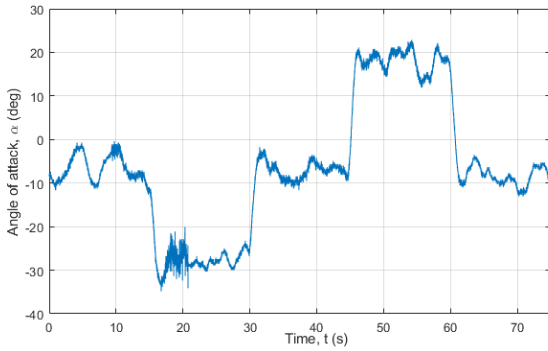


Fig. 19. Wing angle of attack at $\delta_{flap} = \pm 15^\circ$ and $d = 50$ cm

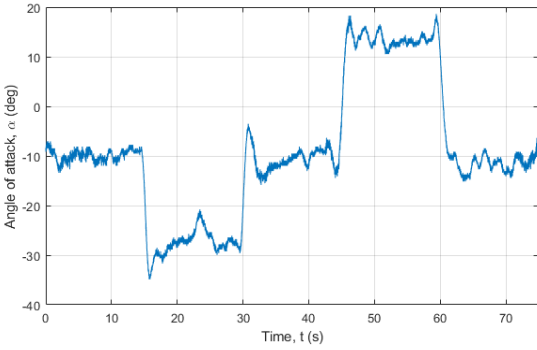


Fig. 20. Wing angle of attack at 15° and $d = 50$ cm

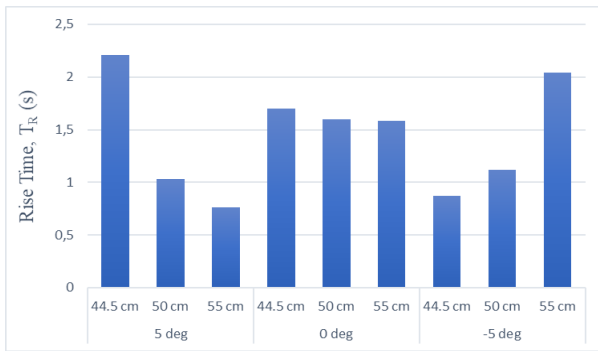


Fig. 21. Recaps of the rise time, T_R at $\delta_{flap} = \pm 5^\circ$

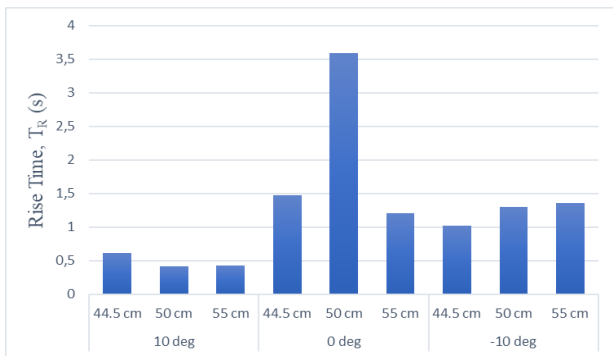


Fig. 22. Recaps of the rise time, T_R at $\delta_{flap} = \pm 10^\circ$

IV. CONCLUSION

The aerodynamic performance of a 1/4th scale wing sail has been experimentally investigated by varying the flap angle in a laboratory set-up. The relation between the flap angle to the wing sail angle of attack has been presented. After constructing the scaled model of the wing, a rotary

encoder sensor, potentiometer and anemometer are installed. The data acquisition was performed using Arduino Uno connected a PC in real-time with Matlab/Simulink.

The experiment shows that there is an almost symmetric response in the angle of attack for the given flap angle. The small discrepancies in the response may be caused by the inaccuracies in the fabrication of the wing sail and construction of the test bench, and the unsteadiness of the generated wind from the electric fan. However, this study presents a quite reasonable characteristic of the resultant forces needed to move the autonomous boat.

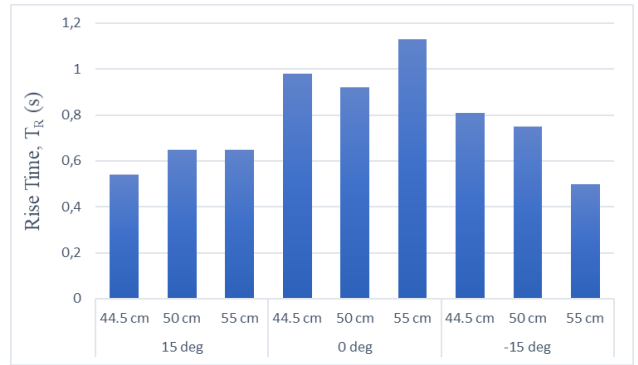


Fig. 23. Recaps of the rise time, T_R at $\delta_{flap} = \pm 15^\circ$

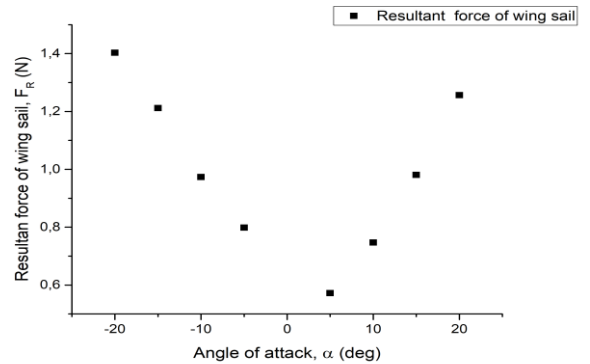


Fig. 24. Measurement result of the resultant force on wing sail

ACKNOWLEDGMENT

This paper was partially supported by the Directorate of Research and Community Service, Ministry of Research, Technology and Higher Education Fiscal Year 2019, and the USAID through Sustainable Higher Education Research Alliances (SHERA) Program-Centre for Collaborative Research (CCR) National Center for Sustainable Transportation Technology (NCSTT).

REFERENCES

- [1] J. Alves, T. Ramos, and N. Cruz, "A reconfigurable computing system for an autonomous sailboat," in *International Robotic Sailing Conference*, 2008, pp. 13–20.
- [2] C. Tretow, "Design of a free-rotating wing sail for an autonomous sailboat," KTH Royal Institute of Technology, 2017.
- [3] B. D. Anderson, "The physics of sailing," *Physics Today*, pp. 38–43, 2008.
- [4] Y. A. Cengel and J. M. Cimbala, *Fluid Mechanics*, 1st ed. New York: McGraw-Hill, 2006.

- [5] L. Du, A. Berson, and R. G. Dominy, "Aerofoil behaviour at high angles of attack and at Reynolds numbers appropriate for small wind turbines," *Mech. Eng. Sci.*, vol. 0, pp. 1–16, 2014.
- [6] N. S. Nise, *Control Systems Engineering*, 7th ed. Pomona: John Wiley & Sons, Inc., 2015.
- [7] A. S. Morris and R. Langari, *Measurement and Instrumentation Theory and Application*, 1st ed. Elsevier, 2012.
- [8] C. Kleijn, "Introduction to Hardware-in-the-Loop Simulation," *ControlLab*, Enschede, pp. 1–15.